HOKKAIDO UNIVERSITY

Title	Virtual states in the complex scaling method
Author(s)	Katō, Kiyoshi; Odsuren, Myagmarjav; Myo, Takayuki et al.
Description	PROCEEDINGS OF THE 4TH INTERNATIONAL WORKSHOP ON “STATE OF THE ART IN NUCLEAR CLUSTER PHYSICS” (SOTANCP4) 13-18 May 2018 Texas, USA
Citation	AIP Conference Proceedings, 2038, 020023 https://doi.org/10.1063/1.5078842
Issue Date	2018-11-13
Doc URL	https://hdl.handle.net/2115/89228
Rights	Copyright 2018 American Institute of Physics. This article may be downloaded for personal use only. Any other use requires prior permission of the author and the American Institute of Physics. The following article appeared in AIP Conf. Proc., 2018, Volume 2038, 020023, and may be found at https://dx.doi.org/10.1063/1.5078842
Type	conference paper
File Information	AIP_020023_1_online.pdf

Hokkaido University Collection of Scholarly and Academic Papers : HUSCAP

AIP Conference Proceedings

RESEARCH ARTICLE | NOVEMBER 13 2018

Virtual states in the complex scaling method

Kiyoshi Katō ✉; Myagmarjav Odsuren; Takayuki Myo; ... et. al

Check for updates

AIP Conference Proceedings 2038, 020023 (2018)
https://doi.org/10.1063/1.5078842

View Online Export Citation CrossMark

Articles You May Be Interested In

Continuum Level Density in Complex Scaling Method

AIP Conference Proceedings (November 2005)

Back Matter for Volume 1109

AIP Conference Proceedings (March 2009)

Combined electromagnetic and photoreaction modeling of CLD-1 photobleaching in polymer microring resonators

Appl. Phys. Lett. (August 2005)

Time to get excited.
Lock-in Amplifiers – from DC to 8.5 GHz

Find out more
Zurich Instruments

AIP Publishing

Downloaded from http://pubs.aip.org/aip/acp/article-pdf/doi/10.1063/1.5078842/14171769/020023_1_online.pdf

Virtual States in the Complex Scaling Method

Kiyoshi Katō[1,a)], Myagmarjav Odsuren[2], Takayuki Myo[3,4], Hiroshi Masui[5] and Yuma Kikuchi[6]

[1]*Nuclear Data Center, Faculty of Science, Hokkaido University, Sapporo 060-0810, Japan*
[2]*School of Engineering and Applied Sciences, Nuclear Research Center, National University of Mongolia, Ulaanbaatar 210646, Mongolia*
[3]*General Education, Faculty of Engineering, Osaka Institute of Technology, Osaka 535-8585, Japan*
[4]*Research Center for Nuclear Physics (RCNP), Osaka University, Ibaraki 567-0047, Japan*
[5]*Information Processing Center, Kitami Institute of Technology, Kitami 090-8507, Japan*
[6]*Department of Physics, Osaka City University, Osaka 558-8585, Japan*

[a)]Corresponding author: kato@nucl.sci.hokudai.ac.jp

Downloaded from http://pubs.aip.org/aip/acp/article-pdf/doi/10.1063/1.5078842/14171769/020023_1_online.pdf

Abstract. A virtual state plays an important role in reaction cross sections just above the breakup threshold energy, such as producing the peak behaviour. However, the virtual state cannot be directly obtained as an isolated pole solution in the complex scaling method (CSM) because of a limit of the scaling angle in the CSM. Recently, we proposed a useful approach to find the pole position of the virtual state using the continuum level density (CLD), the scattering phase shift, and scattering length calculated in the CSM [4]. On the basis of the proposed method, we investigate the photo-disintegration cross sections of resonance and virtual states above the threshold energy to see their differences.

INTRODUCTION

Nuclear states observed around threshold energies provide us with interesting problems associated with nuclear cluster structure. Most of them are also interested astrophysically from the viewpoint of nucleosynthesis. The Hoyle state of the excited 0^+ in ^{12}C is one of typical examples in light nuclei. The first excited $J^\pi = 1/2^+$ state in ^{9}Be, which is an $\alpha+\alpha+n$ Borromean nuclei, offers us the similar problem as well. The first excited $1/2^+$ state in ^{9}Be has been observed as a sharp peak above the ^{8}Be+n threshold energy in the photo-disintegration cross section of $\gamma+^9\text{Be}\rightarrow \alpha+\alpha+n$. Since the size of the peak has a strong influence on the reaction rate of the ^{9}Be synthesis, new experimental data have been investigated recently [1, 2].

We performed calculations using an $\alpha+\alpha+n$ three-cluster model together with the complex scaling method (CSM), which well reproduces the recently-observed photo-disintegration cross section [3, 4]. The results indicate that the virtual state character of the $1/2^+$ state plays an important role in formation of the peak structure appearing in the cross section observed above the ^{8}Be+n threshold. However, the virtual state cannot be directly obtained as an isolated pole solution in the CSM, because the scaling angle in the CSM cannot be increased over the position of the virtual state pole on the negative imaginary axis of the complex momentum plane [5]. A new approach for the CSM to describe the virtual state is needed, and we here discuss a useful approach to find the pole position of the virtual state using the continuum level density (CLD), the scattering phase shift, and scattering length calculated in the CSM [6]. Using the present method, we also discuss the difference in the shapes of the photo-disintegration cross sections of resonant and virtual states.

For this purpose, we apply the CSM to a two-body model, which simulates a ^{8}Be+n model. This model describes the p- and s-state neutron motions around the ^{8}Be cluster corresponding to the ground and first excited states of ^{9}Be, respectively. Changing the strength of the n-^{8}Be potential, we reproduce resonant or virtual state. From results obtained in the calculation, we investigate the accurate position of the virtual state in the CSM and the $E1$ transition strength from the p-wave ground state to the s-wave excited state involving the contribution of the virtual state.

Proceedings of the 4th International Workshop on "State of the Art in Nuclear Cluster Physics" (SOTANCP4)
AIP Conf. Proc. 2038, 020023-1–020023-6; https://doi.org/10.1063/1.5078842
Published by AIP Publishing. 978-0-7354-1764-9/$30.00

METHOD

We solve the Schrödinger equation applying the complex scaling method (CSM):

$$\hat{H}^{\theta}\Psi^{\nu}_{J}(\theta) = E^{\theta}_{\nu}\Psi^{\nu}_{J}(\theta), \tag{1}$$

where J is the total spin and ν is the state index. The complex-scaled Hamiltonian and wave function are given as

$$\hat{H}^{\theta} = U(\theta)\hat{H}U^{-1}(\theta) \qquad \text{and} \qquad \Psi^{\nu}_{J}(\theta) = U(\theta)\Psi^{\nu}_{J}, \tag{2}$$

respectively. The complex scaling operator $U(\theta)$ transforms the relative coordinate $\mathbf{r}$ as

$$U(\theta): \quad \mathbf{r} \rightarrow \mathbf{r}\exp(i\theta), \tag{3}$$

where θ is the scaling angle being a positive real number.

To simulate the relative motion of the ^{8}Be+n system, we employ the Hamiltonian $\hat{H}$ like

$$\hat{H} = -\frac{\hbar^2}{2\mu}\nabla^2_r + V(r). \tag{4}$$

For simplicity, we use $\frac{\hbar^2}{\mu} = 1$ and assume that the interaction potential without the spin-orbit term is $V(r) = V_0\exp(-ar^2)$ with $a = 0.16$ fm^{-2}. The Schrödinger equation (1) can be easily solved by using a basis function expansion with a finite number N for the wave function:

$$\Psi^{\nu}_{\ell}(\theta) = \sum_{n=1}^{N} c^{\ell,\nu}_{n}(\theta)\phi^{\ell}_{n}(\mathbf{r}), \tag{5}$$

where we neglected the spin of the neutron ($J = \ell$). As basis functions, we employ the different-range Gaussian wave functions [7]

$$\phi^{\ell}_{n}(\mathbf{r}) = N^{\ell}_{n}\varphi_{n}(r)Y_{\ell m}(\hat{\mathbf{r}}), \qquad \{\varphi_{n}(r) = r^{\ell-1}\exp(-r^2/2b^2_n) \quad \text{and} \quad b_n = b_0\gamma^{n-1} \quad \text{for} \quad n = 1, 2, \cdots, N\}. \tag{6}$$

N^{ℓ}_{n} and $Y_{\ell m}(\hat{\mathbf{r}})$ are the normalisation factor and the spherical harmonics, respectively. Expansion parameters b_0, γ and N are chosen appropriately so as to obtain well-converged solutions.

Solving the eigenvalue problem, we obtain energies and wave functions; $\{E^{\theta}_{\nu}, \Psi^{\nu}(\theta); \ \nu = 1, 2, \cdots, N\}$. The energies of complex numbers in the CSM are generally classified to three groups; bound-state energies (E_b; real and < 0), resonant-state energies ($E_r = E^R_r - \frac{i}{2}\Gamma_r$, where $\tan^{-1}(\Gamma/(2E^R_r)) < 2\theta$) and continuum-state energies ($E^{\theta}_{c} = E^R_c - iE^I_c$). Here, it is worthwhile to note that E_b and E_r are independent from θ while θ-dependent E_c are obtained along the 2θ-line in the complex energy plane [5]. Using the energy solutions (E^{θ}_{ν}, $E^{\theta}_{0\nu}$) of the Hamiltonian $\hat{H}(\theta)$ (Eq. (4)) and the free-Hamiltonian $\hat{H}_0(\theta)$ without potential terms, we can construct the continuum level density (CLD) $\Delta(E)$:

$$\Delta(E) = \rho(E) - \rho_0(E) = \left\{-\frac{1}{\pi}Im\sum_{\nu}^{N}\frac{1}{E - E^{\theta}_{\nu}}\right\} - \left\{-\frac{1}{\pi}Im\sum_{\nu}^{N}\frac{1}{E - E^{\theta}_{0\nu}}\right\}. \tag{7}$$

From the CLD, the phase shift $\delta(E)$ is calculated as

$$\delta(E) = \pi\int_{0}^{E}\Delta(E')dE'. \tag{8}$$

Assuming a dominant electric-dipole transition described by the operator $\hat{O}(E1)$, we can calculate the photo-disintegration cross section:

$$\sigma^{\gamma}_{E1}(E_\gamma) = \frac{16\pi^3}{9}\left(\frac{E_\gamma}{\hbar c}\right)\frac{dB(E1; E_\gamma)}{dE_\gamma}, \tag{9}$$

where the transition strength is expressed [5] as

$$\frac{dB(E1; E\gamma)}{dE_\gamma} = -\frac{1}{\pi}\frac{1}{2J_{gs}+1}Im\left[\sum_{\nu}^{N}\langle\tilde{\Psi}^{gs}_{J_{gs}}(\theta)\|(\hat{O}^{\theta}(E1))^{\dagger}\|\Psi^{\nu}_{J}(\theta)\rangle\frac{1}{E - E^{\theta}_{\nu}}\langle\tilde{\Psi}^{\nu}_{J}(\theta)\|\hat{O}^{\theta}(E1)\|\Psi^{gs}_{J_{gs}}(\theta)\rangle\right]. \tag{10}$$

Here it should be noticed that a hat of the bra-state indicates the adjoint state for the non-Hermitian Hamiltonian $\hat{H}(\theta)$.

Downloaded from http://pubs.aip.org/aip/acp/article-pdf/doi/10.1063/1.5078842/14171769/020023_1_online.pdf

RESULTS

A. Virtual state

It is believed that the CSM cannot describe virtual states corresponding to S-matrix poles located on the negative imaginary axis on the complex momentum plane. However, in our previous work [3], the peak of the photo-disintegration cross section calculated by using the CSM suggests the existence of the virtual state. To confirm that continuum solutions of the CSM describe the virtual state, we investigate the solutions of the CSM for $J^\pi = 0^+$ and 1^- in more detail.

The energy level diagram of the potential model is shown in Fig. 1 (Left). Here we show the levels of $J^\pi = 0^+$ and 1^-, which are obtained by solving the complex-scaled Schrödinger equation (Eq. (1)). The potential strength V_0 is taken to reproduce one bound $J^\pi = 0^+_1$ of s-waves. But this $J^\pi = 0^+_1$ solution is assumed to be the Pauli forbidden state, because in this model we simulate the ^{8}Be(0^+)+n system which has the Pauli-forbidden ($0s$) neutron configuration. In this model, the 1^-_1 solution describes the ground state. We investigate $E1$ transitions from the 1^- ground state to the excited 0^+ unbound states including the 0^+_2 state. We investigate the behaviour of the $E1$ transition strength as changing the potential strength V_0 for 0^+ and 1^- states.

The pole trajectories for the $J^\pi = 0^+_1$, 1^- and 0^+_2 bound states are shown in Fig. 1 (Right). From the results, we can see that the 0^+_2 state changes from bound to unbound in the range of -1.45 MeV $< V_0 < -1.42$ MeV. For $V_0 = -1.43$ MeV, we obtain the bound 0^+_2 state, but this bound-state solution disappears at $V_0 = -1.42$ MeV. The unbound state for $V_0 = -1.42$ MeV is expected to be a virtual state.

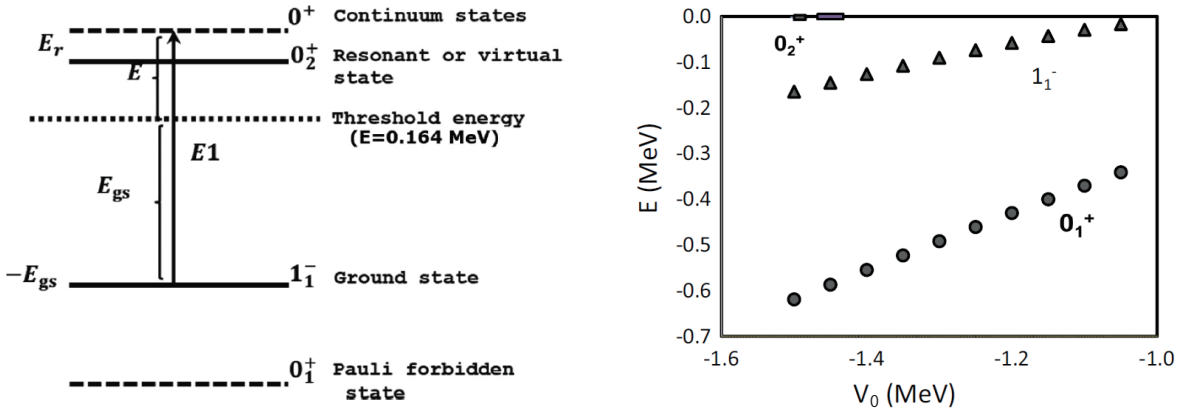

FIGURE 1. Left: The energy level diagram of the two-body potential model simulating ^{9}Be. The dotted line represents the threshold energy. Right: The pole trajectories for the $J^\pi = 0^+_1$ (circles), 1^-_1 (triangles), and 0^+_2 (squares) states calculated as changing the potential strength V_0.

B. Position of a virtual state in the CSM

To see a difference between the calculated CLD's for $V_0 = -1.42$ MeV and -1.43 MeV, we calculate the phase shifts by using solutions of the CSM. The CLD results are presented in Fig. 2 (Left), and we can see a large difference in the low-energy region. In the case of $V_0 = -1.43$ MeV, there is one bound state except for the lowest bound state assigned to the Pauli forbidden state, and then the phase shift (Fig. 2 (Right)) starts from π at $E = 0$ MeV because of the Levinson theorem and decreases with energy. On the other hand, in the case of $V_0 = -1.42$ MeV, the phase shift starts from zero and increases up to about $\pi/3$ but not $\pi/2$ unlike a resonance. This phase shift behavior supports the existence of the virtual state.

We calculate the scattering length a_s from the s-wave phase shift obtained by using the relation

$$a_s = -\lim_{k\to 0} \tan\delta(E)/k, \tag{11}$$

where $k = \sqrt{2\mu E}/\hbar$ is a momentum. For different potential strengths in the range of $-1.43 < V_0 < -1.42$ MeV, the calculated scattering lengths as are shown in Fig. 3. We find a sudden change of a_s in the range of $-1.43 < V_0 < -1.42$

Downloaded from http://pubs.aip.org/aip/acp/article-pdf/doi/10.1063/1.5078842/14171769/020023_1_online.pdf

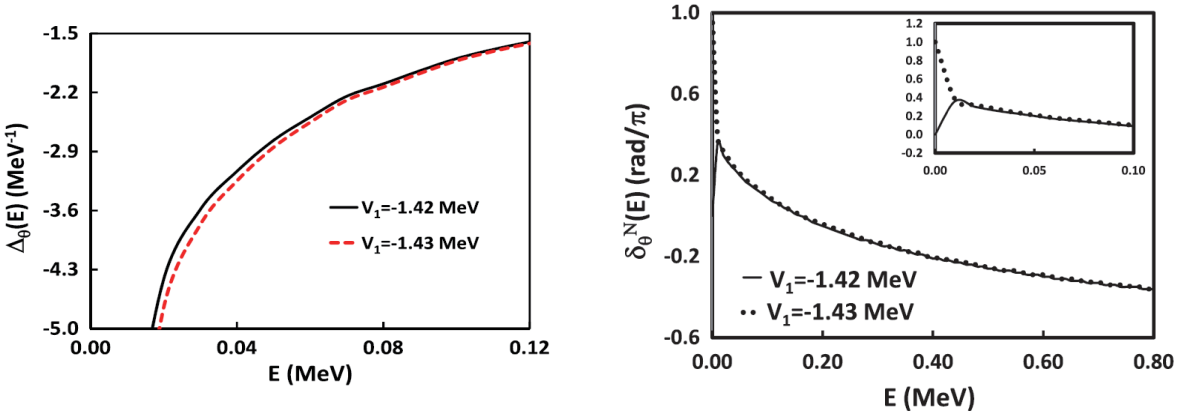

FIGURE 2. Left: Calculated CLD $\Delta(E)$ at the strengths of $V_0 = -1.42$ MeV (solid curve) and -1.43 MeV (dashed curve). Right: Calculated phase shifts $\delta(E)$ of the 0^+ state for $V_0 = -1.42$ MeV (solid curve) and -1.43 MeV (dotted curve). The scale of the graph was magnified in the inset.

MeV. While a_s is positive for the potential strength ($V_0 \leq -1.43$ MeV) reproducing a bound 0_2^+ state, a_s is negative for $V_0 \geq -1.42$ MeV. And at $V_0 = -1.42$ MeV, it is seen that a_s has a large negative value, which also indicates the existence of the virtual state.

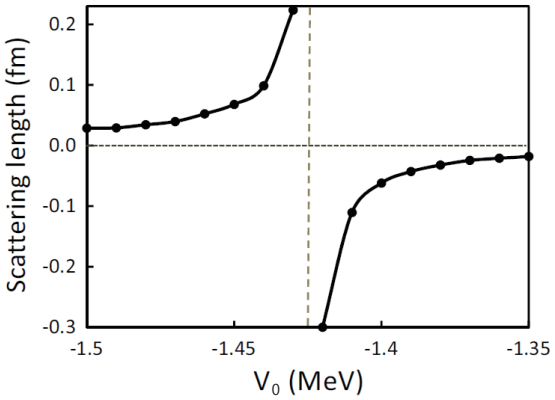

FIGURE 3. Scattering length of the 0^+ state calculated for $V_0 = -1.2$ to -1.5 MeV in the CSM. The horizontal dotted line indicates $a_s = 0$ and the vertical broken line shows a border where a_s changes sign.

We try to extract the virtual-state position in the complex energy plane from the continuum solutions. The CLD $\Delta(E)$ of $J^\pi = 0^+$ states is expected to have a contribution from the virtual state in the case of $V_0 = -1.42$ MeV, which disappears in the case of $V_0 = -1.43$ MeV. In the case of $V_0 = -1.43$ MeV, a bound 0^+ state appears instead of the virtual state, and then the CLD is expressed as

$$\Delta^N(E;\ V_0 = -1.43\,\text{MeV}) = \Delta_b^2(E) + \Delta_c^{N-2}(E;\ V_0 = -1.43\,\text{MeV}), \tag{12}$$

where Δ_b^2 and Δ_c^{N-2} are the contribution from bound-state and continuum-state solutions, respectively. In this case, there are two bound 0^+ states including the Pauli forbidden state, and then the contribution from continuum states is calculated by using the number of $N-2$ continuum solutions along the 2θ-line because of no resonances. In the case of $V_0 = -1.42$ MeV, we have

$$\Delta^N(E;\ V_0 = -1.42\,\text{MeV}) = \Delta_b^1(E) + \Delta_c^{N-1}(E;\ V_0 = -1.42\,\text{MeV}), \tag{13}$$

where the bound 0^+ state is the Pauli forbidden state alone.

Downloaded from http://pubs.aip.org/aip/acp/article-pdf/doi/10.1063/1.5078842/14171769/020023_1_online.pdf

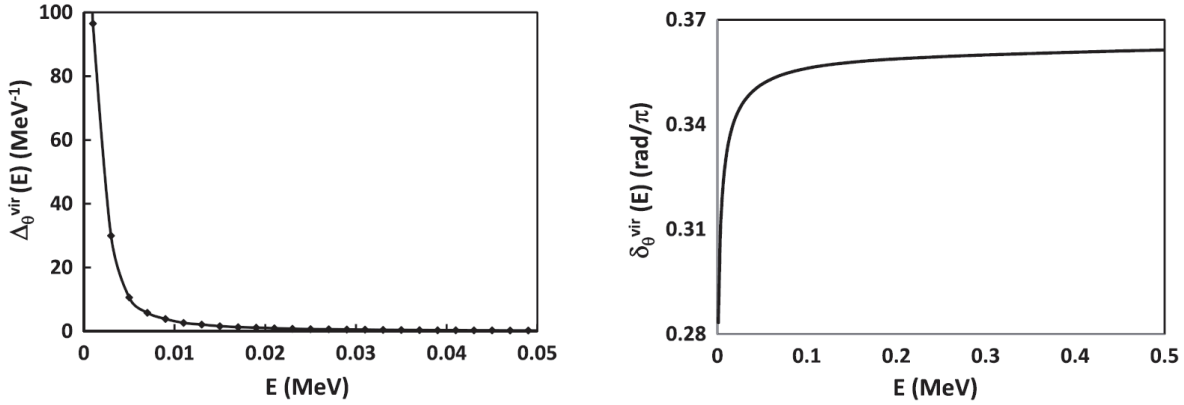

FIGURE 4. Left: The difference $\Delta^{virt}(E)$ between the CLD's for $V_0 = -1.42$ MeV and -1.43 MeV. Right:The phase shift of the virtual state, calculated from the integration of the virtual-state CLD $\Delta^{virt}(E)$.

From these results, we can calculate a difference

$$\Delta^{virt}(E) = \Delta_c^{N-1}(E;\ V_0 = -1.42\,\text{MeV}) - \Delta_c^{N-2}(E;\ V_0 = -1.43\,\text{MeV}). \tag{14}$$

The difference $\Delta^{virt}(E)$ is displayed in Fig. 4 (Left), which shows the sharp peak near the zero energy. Here we assumed that $\Delta_c^{N-1}(E;\ -1.42\ \text{MeV})$ consists of two types of contributions; one is a virtual-state contribution and another is a background. The background contribution was also assumed to have a weak dependence of the strength of V_0. Then the background contributions are considered to be almost the same in both cases of $V_0 = -1.42$ MeV and -1.43 MeV. When the background is expressed by the term of $\Delta_c^{N-2}(E;\ -1.43\ \text{MeV})$ in Eq. (12) approximately, we can consider that $\Delta^{virt}(E)$ corresponds to the virtual-state contribution of the CLD.

Since the phase shift is obtained by integrating the CLD as shown in Eq. (8), the phase shift of the virtual state is given as

$$\delta^{virt}(E) = \pi \int_0^\infty \Delta^{virt}(E')dE'. \tag{15}$$

and the result is presented in Fig. 4 (Right). This result indicates a characteristic behaviour of the phase shift of the virtual state, which is is described by an increasing function of energy but does not reach $\pi/2$. When we assume a negative real energy E_v for the virtual pole, the CLD of the virtual state is considered to be expressed as $\Delta^{virt}(E) \approx 1/(E - E_v)$. Using numerical data shown in Fig. 4 (Left), we can estimate $E_v = -0.001$ MeV.

C. Photo-disintegration cross sections of resonant and virtual states

To reproduce s-wave neutron resonances, we add a long-range repulsive potential artificially as

$$V(r) = -1.42e^{-0.16r^2} + V_2 e^{-0.01r^2}, \tag{16}$$

where the first term makes the virtual state when $V_2 = 0.0$ MeV as discussed above. Increasing values of V_2, we obtained s-wave poles by using the Jost function method [9] and show the trajectory of the complex-energy solutions in Fig. 5 (Left). We can see the resonance solutions are obtained for $V_2 > 0.004$ MeV.

Using the CSM solutions for these potentials with $0 < V_2 \leq 0.01$ MeV, the $E1$ strength functions are calculated and their results are shown in Fig. 5 (Right). The results indicate that the $E1$ strength functions of resonant states obtaind near the zero energy with $V_2 < 0.01$ MeV shows the shape very similar to that of the virtual state though the size of the peaks changes. When $V_2 > 0.01$ MeV, the peak position leaves from the zero-energy region and the shape gradually changes to the Breit-Wigner type for the resonance.

Downloaded from http://pubs.aip.org/aip/acp/article-pdf/doi/10.1063/1.5078842/14171769/020023_1_online.pdf

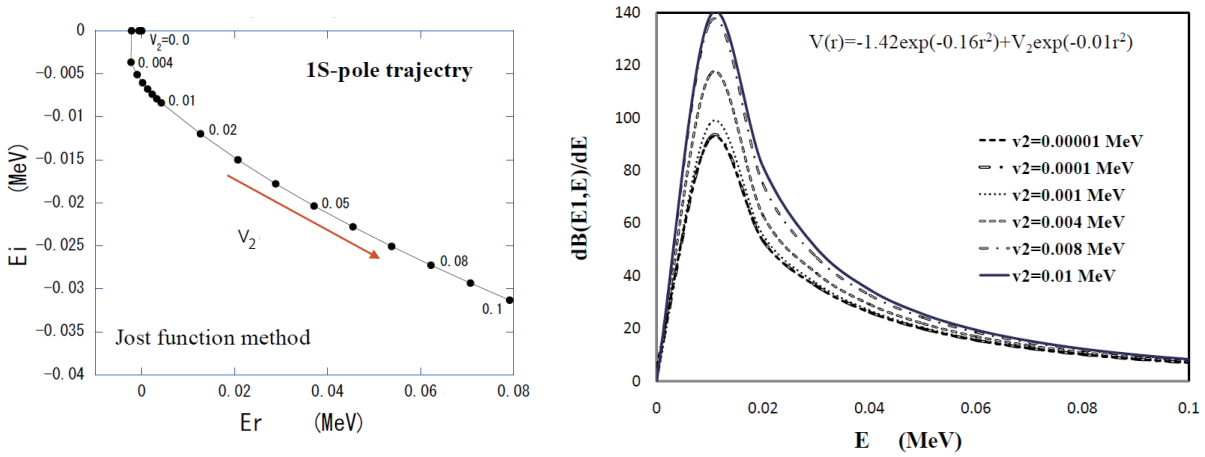

FIGURE 5. Left: The pole trajectory of s-wave states obtained by increasing the strength V_2 of a barrier potential at a large distance. Right: The $E1$ strength functions for the photo-disintegration cross section calculated by using the wave functions of s-waves for different V_2-values in the CSM.

CONCLUSION

The photo-distintegration cross section for the $1/2^+$ state in ^{9}Be shows a peculiar enhancement near the ^{8}Be+n threshold energy and its origin is interesting in relation with the unbound states of ^{9}Be such as virtual state. In this study, simulating the ^{8}Be+n system, we solved the schematic two-body potential model with the CSM in detail.

In the CSM, the virtual state cannot be obtained as an isolated solution, but the continuum solutions are considered to include the effect of the virtual state. We tried to extract the information of the virtual-state pole in terms of the continuum solutions in the CSM. The virtual-state energy E_v obtained by using the CLD was compared with the solution of the Jost function method [9]. The result of very small negative energy of the virtual state is consistent with each other when we employ the basis expansion approach with a finite number of basis states. The $E1$ strength functions for the photo-disintegration cross section of the virtual state has been shown to have the peak just above the threshold energy, which is very similar to that of resonant states near the zero energy. However, in the case of ^{9}Be, it is an open problem to explain the resonance mechanism for an s-wave neutron to be trapped in the inside region of the nucleus.

ACKNOWLEDGMENTS

This work was supported by JSPS KAKENHI Grants No. 25400241 and No.15K05091 and the National University of Mongolia's support for High impact research programm.

REFERENCES

[1] C. W. Arnold, T. B. Clegg, C. Iliadis, H. J. Karwowski, G. C. Rich, J. R. Tompkins, and C. R. Howell, Phys. Rev. C **85**, 044605 (2012).
[2] H. Utsunomiya, S. Katayama, I. Gheorghe, S. Imai, H. Yamaguchi, D. Kahl, Y. Sakaguchi, T. Shima, K. Takahisa, and S. Miyamoto, Phys. Rev. C **92**, 064323 (2015).
[3] M. Odsuren, Y. Kikuchi, T. Myo, M. Aikawa and K. Katō, Phys. Rev. C **92**, 014322 (2015).
[4] Y. Kikuchi, M. Odsuren, T. Myo and K. Katō, Phys. Rev. C **93**, 054605 (2016).
[5] T. Myo, Y. Kikuchi, H. Masui and K. Katō, Prog. Part. Nucl. Phys. **79** (2014), 1.
[6] M. Odsuren Y. Kikuchi, T. Myo, G. Khuukhenkhuu, H. Masui and K. Katō, Phys. Rev. C **95**, 064305 (2017).
[7] E. Hiyama, Y. Kino, and M. Kamimura, Prog. Part. Nucl. Phys. **51**, 223 (2003).
[8] J. R. Taylor, Scattering Theory (JohnWiley & Sons, New York, 1972).
[9] H. Masui, S. Aoyama, T. Myo, K. Katō, and K. Ikeda, Nucl. Phys. **A 673**, 207 (2000).

Downloaded from http://pubs.aip.org/aip/acp/article-pdf/doi/10.1063/1.5078842/14171769/020023_1_online.pdf